# α and 2α decay of nuclei in the region 94 ⩽ Z ⩽ 101 using the modified generalized liquid drop model

Megha Chandran[1] and K. P. Santhosh[1,2,*]

[1]*Department of Physics, University of Calicut, Kerala 673635, India*
[2]*School of Pure and Applied Physics, Kannur University, Swami Anandatheertha Campus, Payyanur, Kerala 670327, India*

The α decay and 2α decay of various isotopes of Pu, Am, Cm, Bk, Cf, Es, Fm, and Md in the mass region $A = 218$ to 273 are investigated using the modified generalized liquid drop model (MGLDM) and universal decay law. The comparison of experimental alpha decay half-lives with the predicted half-lives proves the consistency of our calculations. As a result we broadened our investigation to also include a study of double alpha decay of these isotopes. There is a considerable interest in performing research on double alpha decay, as seen by the proposal submitted at CERN to investigate the double alpha radioactivity of $^{224}$Ra. In view of this, the decay half-lives of most probable 2α emitters, calculated using MGLDM by employing different preformation factors, are presented which can be beneficial for upcoming experimental investigations on this topic. A peak or dip in α and 2α decay half-life is witnessed which indicates the stability of parent or daughter isotopes correspondingly. Minimum and maximum half-lives for decay are observed when the daughter and parent nuclei, respectively, contain a magic number of neutrons. From our study, 126 and 162 are found as magic/semimagic numbers. A linear plot is obtained while plotting $\log_{10} T_{1/2}$ of all the isotopes against $ZQ^{-1/2}$, which emphasizes that our estimations are reliable.

## I. INTRODUCTION

α decay is one of the most significant processes by which an unstable radioactive nucleus decays in the heavy and super-heavy regions. The type of decay associated with the emission of a single alpha particle from massive nuclides has received extensive research attention. Multiple theoretical models are suggested to study single α decay as well as continuous sequential α decay of radioactive nuclei [1–3].

Different forms of decay of atomic nuclei accompanied by the simultaneous emission of two particles of the same kind such as double beta ($2\beta$) decay [4], double gamma ($2\gamma$) decay [5], and two proton ($2p$) [6] and two neutron ($2n$) [7] radioactivities are well known today. Similarly, there is a possibility of simultaneous emission of two alpha particles from a heavy nucleus. This process is known as double alpha ($2\alpha$) decay. In 1985, Poenaru and Ivascu [8] initially suggested the idea of spontaneous and simultaneous emission of $2\alpha$ particles. Nevertheless, $2\alpha$ decay was not explored with much interest like $2\beta$, $2\gamma$, $2p$, and $2n$ radioactivities. Lately this topic has started drawing the attention of many researchers. Tretyak [9] investigated the process of double alpha decay of 80 naturally abundant nuclei in 2021. Utilizing the data from the experiment carried out by de Marcillac et al. [10], the author also predicted the experimental half-life limit for $2\alpha$ emission from $^{209}$Bi as $T_{1/2} > 2.9 \times 10^{20}$ years. A microscopic computation of half-lives for $2\alpha$ decays of $^{212}$Po and $^{224}$Ra was performed by Mercier et al. [11], and the calculated

half-lives were found to be of the order of those observed for cluster emission. Santhosh and Tinu [12] estimated the $2\alpha$ half-life of $^{209}$Bi using the SemFIS formula and compared it with the experimental half-life limit reported by Tretyak. They also computed $2\alpha$ half-lives for different isotopes with atomic numbers varying between 85 and 93 and most of the predicted half-lives were below the measurable upper limit thereby paving a way for experimental investigations in the future. Denisov [13] presented a model for the calculation of the double alpha decay half-life of spherical even-even nuclei and estimated the smallest values of the half-lives of the double α decay of different nuclei. He inferred that the half-lives of double alpha decay are much smaller than the emission of the $^{8}$Be cluster with sequential decay of $^{8}$Be into two α particles. A proposal exists for an experimental probe of the double α decay with $^{224}$Ra on the ISOLDE facility in CERN [14].

The generalized liquid drop model of Royer and Remaud [15,16] is modified by incorporating the proximity 77 potential by Blocki et al. [17], in the well-known theoretical model known as the modified generalized liquid drop model (MGLDM), which was developed by Santhosh et al. [18]. The MGLDM was designed with the aim of carrying out an extensive investigation on the decay half-lives of radioactive nuclei in the heavy and superheavy regions [19,20]. After examining several works [21–23], it is possible to conclude that MGLDM with a preformation factor can be regarded as an efficient mechanism for replicating the experimental half-lives of α and cluster decay. Since half-lives of nuclei can be counted as fundamental properties, a model that can determine the double α half-life will serve as a motivation for additional experimental

---

*drkpsanthosh@gmail.com

studies related to double alpha decay. In this paper, we study both alpha and double alpha decay of different isotopes of elements with atomic numbers ranging from 94 (Pu) to 101 (Md) by using MGLDM with various preformation factors. Section II describes the theory of MGLDM and includes expressions for various preformation factors. The results of the work are presented in Sec. III of the paper. Section IV gives the summary of the entire paper.

## II. THEORY

### A. Modified generalized liquid drop model

In MGLDM, the macroscopic energy for a deformed nucleus is defined as

$$E = E_V + E_S + E_C + E_R + E_P. \qquad (1)$$

Here the terms $E_V$, $E_S$, $E_C$, $E_R$, and $E_P$ represent the volume, surface, Coulomb, rotational, and proximity energy terms, respectively.

The volume, surface, and Coulomb energies in MeV, for the prescission zone, are provided by Royer and Remaud [15] as

$$E_V = -15.494(1 - 1.8I^2)A, \qquad (2)$$

$$E_S = 17.9439(1 - 2.6I^2)A^{2/3}(S/4\pi R_0^2), \qquad (3)$$

$$E_C = 0.6e^2(Z^2/R_0) \times 0.5 \int (V(\theta)/V_0)(R(\theta)/R_0)^3 \sin\theta \, d\theta. \qquad (4)$$

Here $I$ is the relative neutron excess, $S$ is the surface of the deformed nucleus, $V(\theta)$ is the electrostatic potential at the surface, and $V_0$ is the surface potential of the sphere.

For the postscission region [15],

$$E_V = -15.494[(1 - 1.8I_1^2)A_1 + (1 - 1.8I_2^2)A_2], \qquad (5)$$

$$E_S = 17.9439[(1 - 2.6I_1^2)A_1^{2/3} + (1 - 2.6I_2^2)A_2^{2/3}], \qquad (6)$$

$$E_C = \frac{0.6e^2Z_1^2}{R_1} + \frac{0.6e^2Z_2^2}{R_2} + \frac{e^2Z_1Z_2}{r}. \qquad (7)$$

Here $A_i$, $Z_i$, $R_i$, and $I_i$ are the masses, charges, radii, and relative neutron excess of the fragments, $r$ is the distance between the centers of the fragments, and

$$E_p(z) = 4\pi\gamma b \left[\frac{C_1 C_2}{(C_1 + C_2)}\right] \Phi\left(\frac{z}{b}\right) \qquad (8)$$

is the nuclear proximity potential of Blocki et al. [17] with $\gamma$ the nuclear surface tension coefficient and $\Phi$ the universal proximity potential [24].

The barrier penetrability $P$ is calculated using the following integral [15]:

$$P = \exp\left\{-\frac{2}{\hbar}\int_{R_{in}}^{R_{out}}\sqrt{2B(r)[E(r) - E(\text{sphere})]}dr\right\}, \qquad (9)$$

Where $R_{in} = R_1 + R_2$, $B(r) = \mu$ and $R_{out} = e^2Z_1Z_2/Q$. $R_1$, $R_2$ are the radius of the daughter nuclei and emitted cluster, respectively, $\mu$ is the reduced mass, and $Q$ is the released energy.

The partial half-life is related to the decay constant $\lambda$ by

$$T_{1/2} = \left(\frac{\ln 2}{\lambda}\right) = \left(\frac{\ln 2}{\nu P_C P}\right). \qquad (10)$$

The assault frequency $\nu$ has been taken as $10^{20} \text{ s}^{-1}$ and $P_c$ is the preformation factor.

#### 1. Preformation factor

We suppose that the $2\alpha$ particle is already generated within the parent nucleus prior to emission, much like in alpha and cluster decay. It is important to highlight that the decay half-life is greatly influenced by the variables on which preformation depends. In earlier works [20–23], various preformation factors were developed to study alpha and cluster decay. Due to the simultaneous emission of both alpha particles during double alpha decay, one can envision a scenario in which $2\alpha$ particles are formed, pass through the potential barrier as a cluster, and then tunnel through the nucleus to become emitted as two $\alpha$ particles. Preformation factors that depend on $Q$ value, cluster size, atomic number of cluster and daughter nuclei, and the combination of these three parameters were used to calculate alpha and cluster half-life. Thus, MGLDM with various preformation variables that demonstrated its application in the alpha and cluster decay can be viewed as an appealing concept to explain the concept of emission of double alpha particles, and the preformation parameters are as follows.

(1) A preformation factor that depends on Q value is

$$P_c(Q) = 10^{aQ+bQ^2+c}, \qquad (11)$$

with $a = -0.257\,36$, $b = 6.372\,91 \times 10^{-4}$, and $c = 3.351\,06$.

(2) A preformation factor that depends on cluster size is

$$P_c(A_c) = 10^{aA_c+b}, \qquad (12)$$

with $a = -0.513\,25$ and $b = 2.807\,87$

(3) A preformation factor that depends on proton number of cluster and daughter nuclei is

$$P_c(Z_c Z_d) = 10^{aZ_c Z_d + b}, \qquad (13)$$

with $a = -0.015\,55$ and $b = 3.229\,40$

(4) A preformation factor that depends on the combined effect of $Q$ value, cluster size, and proton number of cluster and daughter nuclei is

$$P_c(C) = 10^{aA_c + bZ_c Z_d + cQ + dQ^2 + e}, \qquad (14)$$

with $a = -0.5559$, $b = 0.028\,716$, $c = -0.423\,335\,8$, $d = 0.001\,143$, and $e = 1.490\,754$

In the expressions mentioned above for preformation parameters, $Q$, $A_c$, and $Z_c Z_d$ are the $Q$ value, cluster size, and atomic number of cluster and daughter nucleus, respectively. The value of constants in each expression was obtained by least square fitting to the preformation factor extracted from experimentally observed cluster decay data. For this we considered 28 modes of decay from nuclei ranging from Fr to Cm

TABLE I. The $\alpha$ decay half-lives of different isotopes of Pu, Am, Cm, Bk, Cf, Es, Fm, and Md predicted using MGLDM and UDL compared with corresponding experimental data [28].

| Parent nuclei | Emitted cluster | Daughter nuclei | $Q$ Value (MeV) | $\log_{10}[T_{1/2}$ (s)] | | |
|---|---|---|---|---|---|---|
| | | | | Experimental | MGLDM | UDL |
| $^{228}\text{Pu}_{94}$ | $\alpha$ | $^{224}\text{U}_{92}$ | 8.121584 | 0.0414 | −0.5607 | −0.7029 |
| $^{230}\text{Pu}_{94}$ | $\alpha$ | $^{226}\text{U}_{92}$ | 7.377784 | 2.0086 | 2.0379 | 1.7534 |
| $^{236}\text{Pu}_{94}$ | $\alpha$ | $^{232}\text{U}_{92}$ | 5.940584 | 7.9547 | 8.4003 | 7.7331 |
| $^{238}\text{Pu}_{94}$ | $\alpha$ | $^{234}\text{U}_{92}$ | 5.940584 | 9.4420 | 8.3458 | 7.6875 |
| $^{239}\text{Pu}_{94}$ | $\alpha$ | $^{235}\text{U}_{92}$ | 5.669484 | 11.8813 | 9.8421 | 9.0865 |
| $^{240}\text{Pu}_{94}$ | $\alpha$ | $^{236}\text{U}_{92}$ | 5.286984 | 11.3161 | 12.1333 | 11.2231 |
| $^{242}\text{Pu}_{94}$ | $\alpha$ | $^{238}\text{U}_{92}$ | 4.803184 | 13.0719 | 15.4123 | 14.2754 |
| $^{244}\text{Pu}_{94}$ | $\alpha$ | $^{240}\text{U}_{92}$ | 4.587184 | 15.4082 | 17.0261 | 15.7778 |
| $^{229}\text{Am}_{95}$ | $\alpha$ | $^{225}\text{Np}_{93}$ | 8.321284 | 0.2553 | −0.8274 | −0.9347 |
| $^{230}\text{Am}_{95}$ | $\alpha$ | $^{226}\text{Np}_{93}$ | 7.910684 | 1.6021 | 0.5221 | 0.3435 |
| $^{241}\text{Am}_{95}$ | $\alpha$ | $^{237}\text{Np}_{93}$ | 5.750784 | 10.1351 | 9.8592 | 9.1314 |
| $^{243}\text{Am}_{95}$ | $\alpha$ | $^{239}\text{Np}_{93}$ | 5.234084 | 11.3654 | 12.9662 | 12.0307 |
| $^{240}\text{Cm}_{96}$ | $\alpha$ | $^{236}\text{Pu}_{94}$ | 6.787884 | 6.4194 | 5.1705 | 4.7649 |
| $^{242}\text{Cm}_{96}$ | $\alpha$ | $^{238}\text{Pu}_{94}$ | 6.168284 | 7.1482 | 8.0916 | 7.5063 |
| $^{243}\text{Cm}_{96}$ | $\alpha$ | $^{239}\text{Pu}_{94}$ | 5.856184 | 8.9629 | 9.7425 | 9.0512 |
| $^{244}\text{Cm}_{96}$ | $\alpha$ | $^{240}\text{Pu}_{94}$ | 5.624984 | 8.7570 | 11.0515 | 10.2748 |
| $^{245}\text{Cm}_{96}$ | $\alpha$ | $^{241}\text{Pu}_{94}$ | 5.463484 | 11.4155 | 12.0110 | 11.1715 |
| $^{247}\text{Cm}_{96}$ | $\alpha$ | $^{243}\text{Pu}_{94}$ | 5.185984 | 14.6922 | 13.7624 | 12.8068 |
| $^{248}\text{Cm}_{96}$ | $\alpha$ | $^{244}\text{Pu}_{94}$ | 5.103184 | 13.0407 | 14.3063 | 13.3152 |
| $^{247}\text{Bk}_{97}$ | $\alpha$ | $^{243}\text{Am}_{95}$ | 5.836884 | 10.6389 | 10.2873 | 9.5937 |
| $^{240}\text{Cf}_{98}$ | $\alpha$ | $^{236}\text{Cm}_{96}$ | 7.657684 | 1.6053 | 2.5009 | 2.2945 |
| $^{246}\text{Cf}_{98}$ | $\alpha$ | $^{242}\text{Cm}_{96}$ | 6.697884 | 5.1089 | 6.3918 | 5.9694 |
| $^{248}\text{Cf}_{98}$ | $\alpha$ | $^{244}\text{Cm}_{96}$ | 6.430584 | 7.4594 | 7.6309 | 7.1359 |
| $^{249}\text{Cf}_{98}$ | $\alpha$ | $^{245}\text{Cm}_{96}$ | 6.367084 | 10.0444 | 7.9279 | 7.4166 |
| $^{250}\text{Cf}_{98}$ | $\alpha$ | $^{246}\text{Cm}_{96}$ | 6.354884 | 8.6157 | 7.9709 | 7.4594 |
| $^{251}\text{Cf}_{98}$ | $\alpha$ | $^{247}\text{Cm}_{96}$ | 6.362284 | 10.4524 | 7.9158 | 7.4103 |
| $^{252}\text{Cf}_{98}$ | $\alpha$ | $^{248}\text{Cm}_{96}$ | 6.341284 | 7.9215 | 8.0033 | 7.4947 |
| $^{241}\text{Es}_{99}$ | $\alpha$ | $^{237}\text{Bk}_{97}$ | 8.132784 | 0.7076 | 1.1819 | 1.0707 |
| $^{253}\text{Es}_{99}$ | $\alpha$ | $^{249}\text{Bk}_{97}$ | 6.805784 | 6.2476 | 6.2314 | 5.8584 |
| $^{254}\text{Es}_{99}$ | $\alpha$ | $^{250}\text{Bk}_{97}$ | 6.700884 | 7.3769 | 6.6976 | 6.2983 |
| $^{243}\text{Fm}_{100}$ | $\alpha$ | $^{239}\text{Cf}_{98}$ | 8.678584 | −0.6364 | −0.2653 | −0.2767 |
| $^{245}\text{Fm}_{100}$ | $\alpha$ | $^{241}\text{Cf}_{98}$ | 8.519784 | 0.6284 | 0.2073 | 0.1766 |
| $^{246}\text{Fm}_{100}$ | $\alpha$ | $^{242}\text{Cf}_{98}$ | 8.209984 | 0.1875 | 1.2269 | 1.1449 |
| $^{248}\text{Fm}_{100}$ | $\alpha$ | $^{244}\text{Cf}_{98}$ | 7.651984 | 1.5378 | 3.2217 | 3.0347 |
| $^{250}\text{Fm}_{100}$ | $\alpha$ | $^{246}\text{Cf}_{98}$ | 7.349384 | 3.2695 | 4.3854 | 4.1366 |
| $^{252}\text{Fm}_{100}$ | $\alpha$ | $^{248}\text{Cf}_{98}$ | 7.269584 | 4.9609 | 4.6784 | 4.4175 |
| $^{254}\text{Fm}_{100}$ | $\alpha$ | $^{250}\text{Cf}_{98}$ | 7.286184 | 4.0669 | 4.5735 | 4.3236 |
| $^{255}\text{Fm}_{100}$ | $\alpha$ | $^{251}\text{Cf}_{98}$ | 7.161284 | 4.8589 | 5.0806 | 4.8032 |
| $^{257}\text{Fm}_{100}$ | $\alpha$ | $^{253}\text{Cf}_{98}$ | 6.761684 | 6.9387 | 6.8237 | 6.4460 |
| $^{244}\text{Md}_{101}$ | $\alpha$ | $^{240}\text{Es}_{99}$ | 9.284884 | −0.4437 | −1.7347 | −1.6537 |
| $^{245}\text{Md}_{101}$ | $\alpha$ | $^{241}\text{Es}_{99}$ | 9.367684 | 0.4202 | −1.9899 | −1.8943 |
| $^{246}\text{Md}_{101}$ | $\alpha$ | $^{242}\text{Es}_{99}$ | 9.195184 | −0.0362 | −1.5116 | −1.4363 |
| $^{247}\text{Md}_{101}$ | $\alpha$ | $^{243}\text{Es}_{99}$ | 8.883784 | 0.0756 | −0.5956 | −0.5626 |
| $^{258}\text{Md}_{101}$ | $\alpha$ | $^{254}\text{Es}_{99}$ | 7.345384 | 6.6491 | 4.6941 | 4.4676 |

emitting $^{14}$C to $^{34}$Si. To find the accuracies of these formulas we computed the standard deviation of cluster decay half-lives and the values obtained are 1.08, 0.995, 1.07, and 0.885, respectively, for preformation probabilities dependent on $Q$ value, cluster size, product of proton number of cluster and daughter nuclei, and the combination of these three parameters, respectively.

### B. Universal decay law

The expression for the universal decay law (UDL) for cluster decay proposed by Qi *et al.* [25] is given as

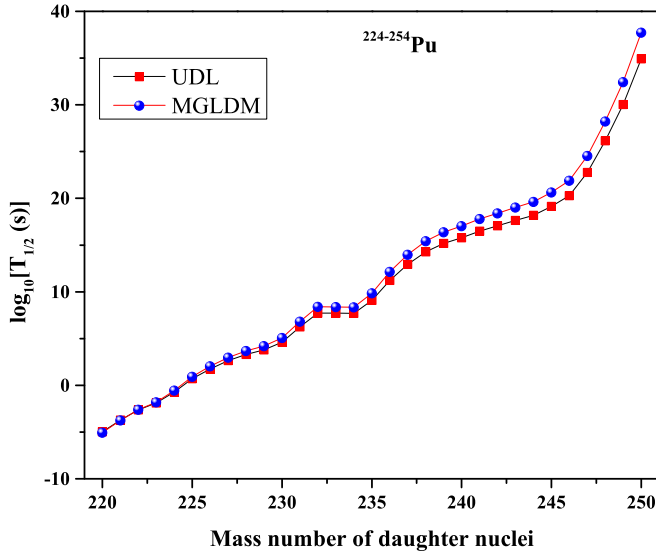$$\log_{10}(T_{1/2}) = aZ_cZ_d\sqrt{A/Q_c} + b\sqrt{AZ_cZ_d\left(A_d^{1/3} + A_c^{1/3}\right)} + c \tag{15}$$

FIG. 1. The variation of logarithm of half-life with the mass number of daughter nucleus for $\alpha$ decay from $^{224-254}$Pu. Blue circle and red square represent the half-life computed using MGLDM and UDL respectively.

where $A_c$, $A_d$, $Z_c$, and $Z_d$ are mass number of cluster, mass number of daughter, proton number of cluster, and proton number of daughter, respectively. The constants are $a = 0.3949$, $b = -0.3693$, $c = -23.7615$, and $A = A_c A_d / (A_c + A_d)$.

## III. RESULTS AND DISCUSSION

The $\alpha$ decay and $2\alpha$ decay of different isotopes of Pu, Am, Cm, Bk, Cf, Es, Fm, and Md in the mass region $A = 218$ to 273 are studied using MGLDM by incorporating different preformation factors. The ejected particle is assumed to
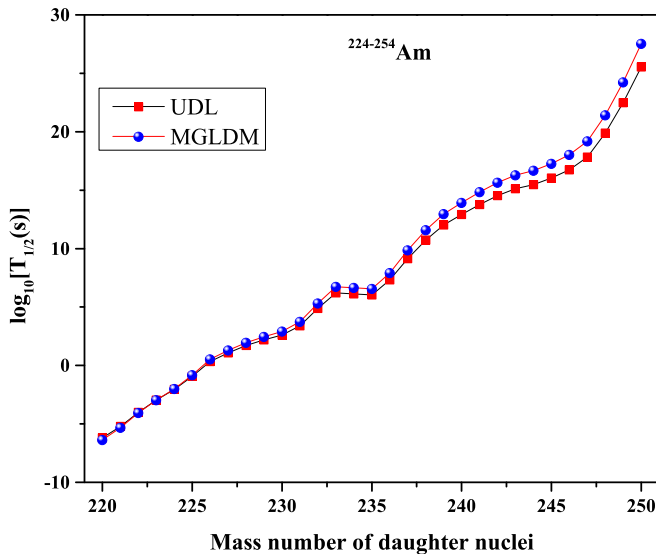


FIG. 2. The variation of logarithm of half-life with the mass number of daughter nucleus for $\alpha$ decay from $^{224-254}$Am.


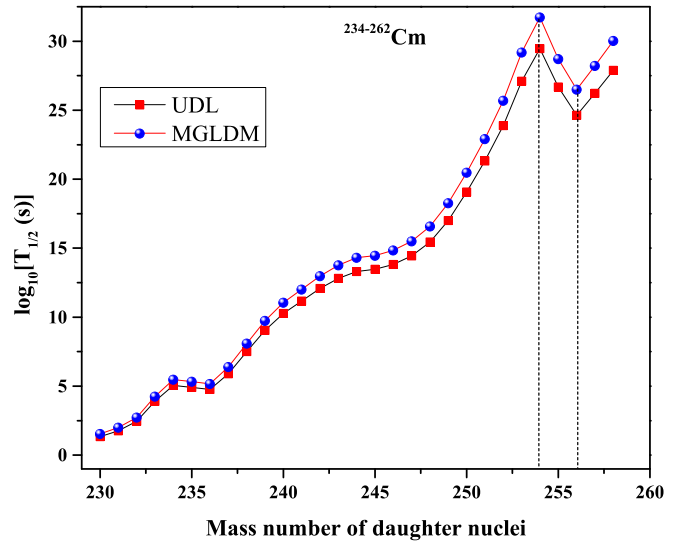
FIG. 3. The variation of logarithm of half-life with the mass number of daughter nucleus for $\alpha$ decay from $^{234-262}$Cm. The dashed lines represent the minimum and maximum half-lives.

tunnel through a potential barrier before being emitted from the radioactive nucleus. As two $\alpha$ particles are simultaneously emitted in $2\alpha$ decay, we can envision a scenario where both the alpha particles move as a cluster and leave the nucleus after overcoming the potential barrier. The $Q$ value of a reaction is given by the equation

$$Q = \Delta M_p - (\Delta M_d + \Delta M_c) \tag{16}$$

where $\Delta M_p$, $\Delta M_d$, and $\Delta M_c$ are the mass excess of parent, daughter, and cluster nuclei, respectively. For $\alpha$ decay $\Delta M_c = \Delta M_\alpha$ and for $2\alpha$ decay $\Delta M_c = 2 \times \Delta M_\alpha$, where $\Delta M_\alpha$ is the mass excess of $\alpha$ particles. The $\alpha$ decay and $2\alpha$ decay are energetically possible only if $Q > 0$. The $Q$ values for the decay of all the isotopes are calculated using the mass excess
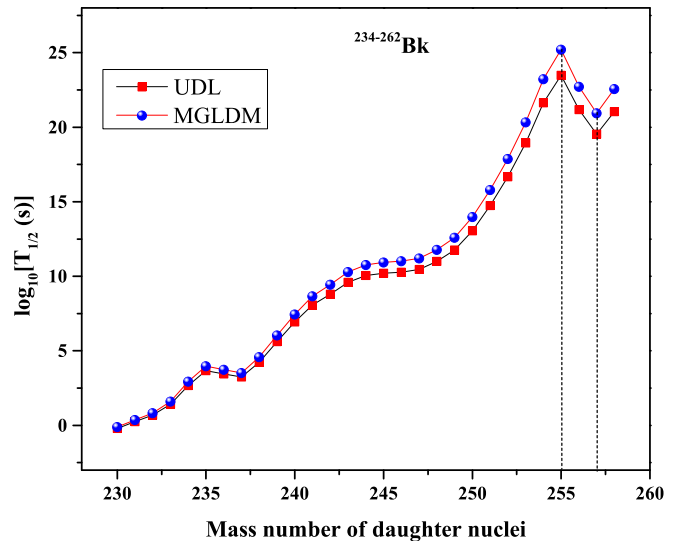


FIG. 4. The variation of logarithm of half-life with the mass number of daughter nucleus for $\alpha$ decay from $^{234-262}$Bk.
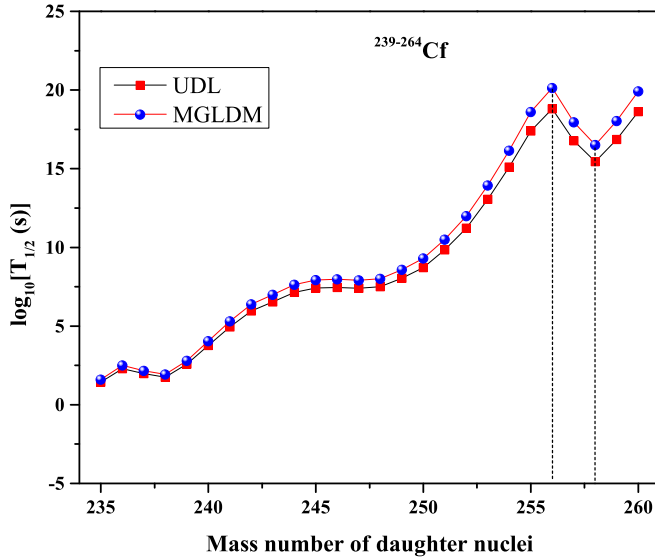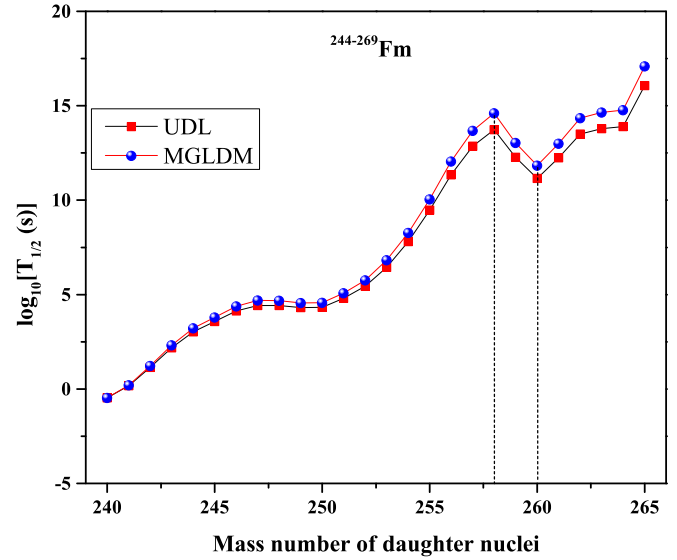
FIG. 5. The variation of logarithm of half-life with the mass number of daughter nucleus for $\alpha$ decay from $^{239-264}$Cf.

values from the WS4 mass table [26]. The mass excess values of the $\alpha$ particle and $^8$Be are taken from the mass table of Wang *et al.* [27].

Table I depicts the comparison of predicted $\alpha$ decay half-lives of various isotopes of Pu, Am, Cm, Bk, Cf, Es, Fm, and Md calculated using MGLDM with preformation factor $P_c = 1$, with the experimental data obtained from Kondev *et al.* [28]. The predicted values are also compared with the values computed using the universal decay law of Qi *et al.* [25].

The standard deviation of the theoretical half-lives from the experimental half-lives is calculated using the



FIG. 6. The variation of logarithm of half-life with the mass number of daughter nucleus for $\alpha$ decay from $^{239-264}$Es.



FIG. 7. The variation of logarithm of half-life with the mass number of daughter nucleus for $\alpha$ decay from $^{244-269}$Fm.

equation

$$\sigma = \sqrt{\frac{1}{N}\sum_{i=1}^{N}\left[\left(\log_{10}T_{1/2}^{\text{theory}} - \log_{10}T_{1/2}^{\text{exp}}\right)^2\right]}. \quad (17)$$

The experimental data and the logarithm of alpha half-life values predicted using MGLDM and UDL agree fairly well, with a standard deviation of 1.18 and 1.20, respectively. This outcome demonstrates that our estimations are valid and reliable. Consequently, we come to the conclusion that double alpha decay can also be researched using this method in order to achieve better results. Figures 1–8 show the variation of logarithms of half-life predicted using MGLDM and UDL
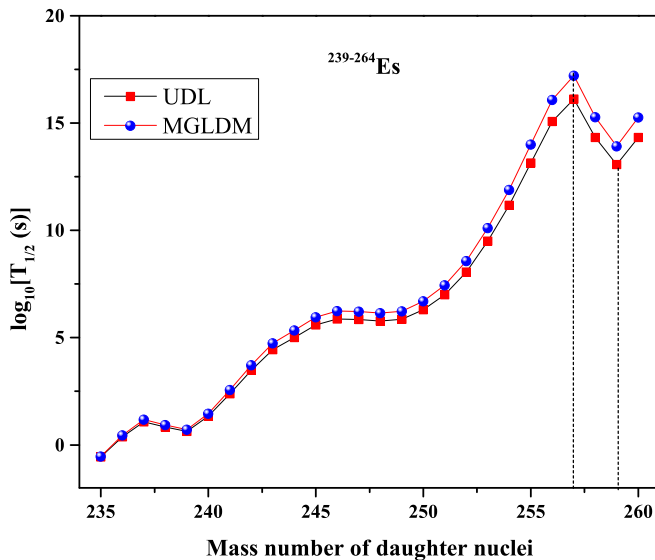


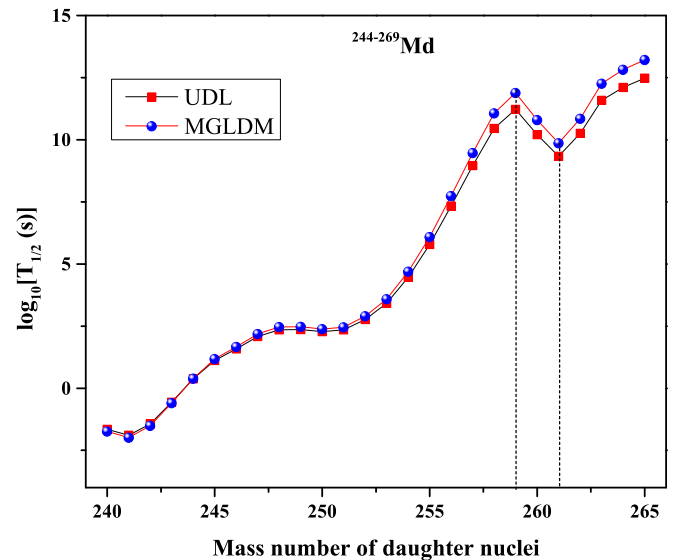FIG. 8. The variation of logarithm of half-life with the mass number of daughter nucleus for $\alpha$ decay from $^{244-269}$Md.

TABLE II. Comparison of half-life predicted using UDL and MGLDM with different preformation factors for $2\alpha$ and $^8$Be emissions.

| Parent nuclei | Emitted cluster | Daughter nuclei | $Q$ Value (MeV) | $\log_{10}[T_{1/2}\,(\text{s})]$ | | | | | |
|---|---|---|---|---|---|---|---|---|---|
| | | | | $T_{1/2}^{\text{MGLDM}}$ | $T_{1/2}^{(Q)}$ | $T_{1/2}^{(A_c)}$ | $T_{1/2}^{(Z_c Z_d)}$ | $T_{1/2}^{(C)}$ | $T_{1/2}^{(\text{UDL})}$ |
| $^{229}$Pu$_{94}$ | $^8$Be | $^{221}$Th$_{90}$ | 15.48403 | 19.073 | 19.554 | 20.371 | 21.442 | 17.973 | 21.398 |
| | $2\alpha$ | | 15.57587 | 18.765 | 19.268 | 20.064 | 21.134 | 17.701 | 21.102 |
| $^{230}$Am$_{95}$ | $^8$Be | $^{222}$Pa$_{91}$ | 16.01253 | 18.091 | 18.698 | 19.389 | 20.522 | 17.080 | 20.491 |
| | $2\alpha$ | | 16.10437 | 17.796 | 18.424 | 19.094 | 20.227 | 16.821 | 20.206 |
| $^{232}$Cm$_{96}$ | $^8$Be | $^{224}$U$_{92}$ | 16.02473 | 18.768 | 19.377 | 20.066 | 21.261 | 17.647 | 21.189 |
| | $2\alpha$ | | 16.11657 | 18.469 | 19.101 | 19.768 | 20.962 | 17.384 | 20.901 |
| $^{234}$Bk$_{97}$ | $^8$Be | $^{226}$Np$_{93}$ | 16.13603 | 19.120 | 19.756 | 20.418 | 21.675 | 17.928 | 21.574 |
| | $2\alpha$ | | 16.22787 | 21.286 | 18.822 | 19.479 | 20.119 | 21.377 | 21.286 |
| $^{236}$Cf$_{98}$ | $^8$Be | $^{228}$Pu$_{94}$ | 16.54053 | 18.526 | 19.257 | 19.824 | 21.143 | 17.374 | 21.045 |
| | $2\alpha$ | | 16.63237 | 18.235 | 18.988 | 19.533 | 20.853 | 17.119 | 20.764 |
| $^{239}$Es$_{99}$ | $^8$Be | $^{231}$Am$_{95}$ | 16.73813 | 18.563 | 19.342 | 19.862 | 21.243 | 17.373 | 21.133 |
| | $2\alpha$ | | 16.82997 | 18.275 | 19.075 | 19.573 | 20.955 | 17.121 | 20.854 |
| $^{241}$Fm$_{100}$ | $^8$Be | $^{233}$Cm$_{96}$ | 17.19803 | 17.826 | 18.713 | 19.124 | 20.568 | 16.698 | 20.464 |
| | $2\alpha$ | | 17.28987 | 17.547 | 18.455 | 18.845 | 20.289 | 16.454 | 20.193 |
| $^{245}$Md$_{101}$ | $^8$Be | $^{237}$Bk$_{97}$ | 17.40863 | 17.794 | 18.730 | 19.092 | 20.598 | 16.632 | 20.489 |
| | $2\alpha$ | | 17.50047 | 17.517 | 18.475 | 18.815 | 20.321 | 16.390 | 20.221 |

with the mass number of daughter nuclei for the $\alpha$ decay from $^{224-254}$Pu, $^{224-254}$Am, $^{234-262}$Cm, $^{234-262}$Bk, $^{239-264}$Cf, $^{239-264}$Es, $^{244-269}$Fm, and $^{244-269}$Md. Only those decays with half-lives up to $10^{40}$ s are plotted in all these figures. The blue circle in the figure represents the predictions of MGLDM whereas the red square represents the UDL predictions. From Fig. 3, which depicts the $\alpha$ decay of $^{234-262}$Cm, we can observe that the half-life is minimum when the mass number of the daughter nuclei is 256. The neutron number of the daughter nucleus corresponding to mass number 256 is 162. We can therefore draw the conclusion that $\log_{10} T_{1/2}$ is minimum for the parent isotope when the daughter nucleus has a magic number of neutrons. A shorter half-life suggests that there is a greater likelihood that the nucleus will disintegrate. The daughter nucleus which possesses a magic number of neutrons will be more stable in comparison with other daughter nuclei formed during $\alpha$ decay. The daughter nucleus will have a high degree of stability when the minimal $\log_{10} T_{1/2}$ value is deeper. The half-life peaks at mass number 254, which corresponds to the parent isotope's neutron number 162. Parent isotopes having a magic number of neutrons show comparatively longer half-life indicating that they are stable against $\alpha$ decay. The parent nuclei's stability grows together with the height of the peak corresponding to maximum $T_{1/2}$ value.

According to Fig. 4, during the $\alpha$ decay of $^{234-262}$Bk, minimum half-life is seen at mass number 257 or more specifically at neutron number 162. Similarly when the parent nuclei's neutron number is 162, corresponding to mass number 255, the half-life is maximum, representing extra stability against the decay. From Fig. 5, we can see that when the daughter nuclei's neutron number is 162 or at mass number 258, minimum $T_{1/2}$ is observed for the $\alpha$ decay of $^{239-264}$Cf. Maximum $T_{1/2}$ occur at mass numbers 256 when the number of neutrons of the parent isotope is 162.

Figure 6 shows that, for the $\alpha$ decay of $^{239-264}$Es, $T_{1/2}$ acquires its lowest value at mass number 259, with neutron number 162, whereas $T_{1/2}$ is at its highest when the mass

number of the daughter (neutron number of the parent) is 257 (162). By analyzing Fig. 7, we can infer that when $^{244-269}$Fm undergoes $\alpha$ decay, the daughter nucleus has minimum $T_{1/2}$ at mass number 260 when the neutron number of the daughter is 126. Due to the magicity of the parent nuclei, maximum half-life is exhibited when the mass number of the daughter is 258, where the corresponding neutron number of the parent is 162. As shown in Fig. 8, for the $\alpha$ decay of $^{244-269}$Md, the least half-life is obtained at mass number 261 corresponding to magic neutron number 162, while the half-life peaks at mass number 259 when the parent nuclei's neutron number is 162.

By examining all these graphs, we can conclude that the magicity of the neutron number plays a crucial role in the decay process of all these isotopes. The half-life is at its
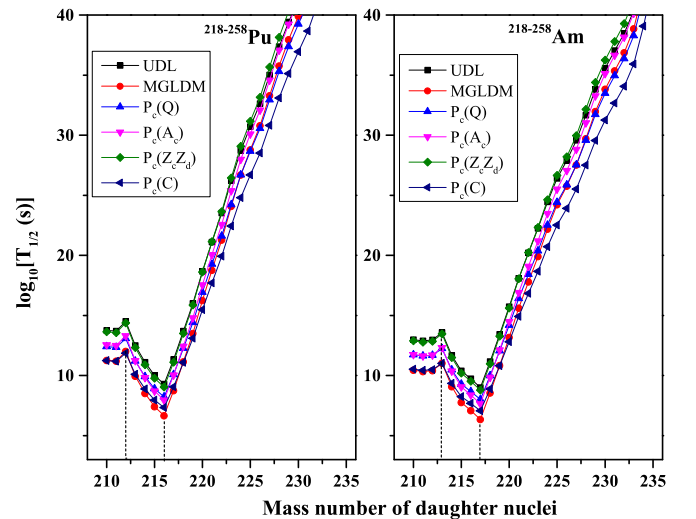


FIG. 9. The variation of logarithm of half-life with the mass number of daughter nucleus for $2\alpha$ decay from $^{218-258}$Pu and $^{218-258}$Am.
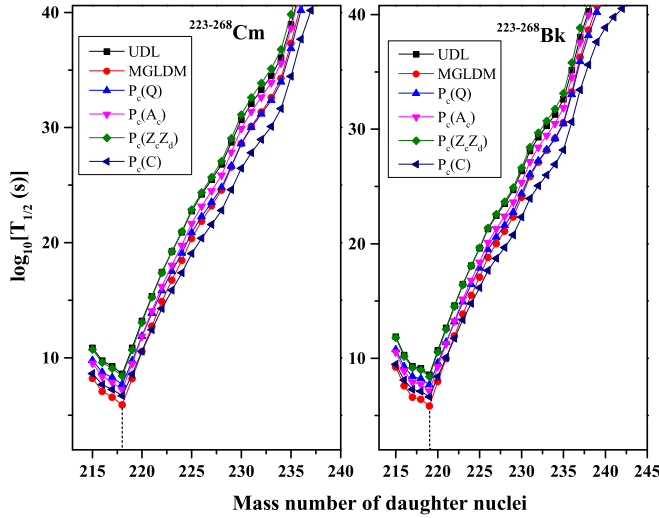
FIG. 10. The variation of logarithm of half-life with the mass number of daughter nucleus for $2\alpha$ decay from $^{223-268}$Cm and $^{223-268}$Bk.



FIG. 12. The variation of logarithm of half-life with the mass number of daughter nucleus for $2\alpha$ decay from $^{238-273}$Fm and $^{238-273}$Md.

minimum when the daughter nucleus possesses a magic number of neutrons. Since daughter nuclei with magic number of neutrons are more stable, the parent nuclei readily emit an alpha particle to create them. Such processes will proceed very easily when compared to other decay and hence exhibit a minimum half-life. However when the parent nuclei contain a magic number of neutrons they will not be ready to destroy their stable configuration by undergoing decay. These processes take longer to complete because they are resistant to decay, giving them maximum half-life. In general, a minimum half-life symbolizes the magicity of the daughter nucleus whereas maximum half-life represents the magicity of the parent nucleus.
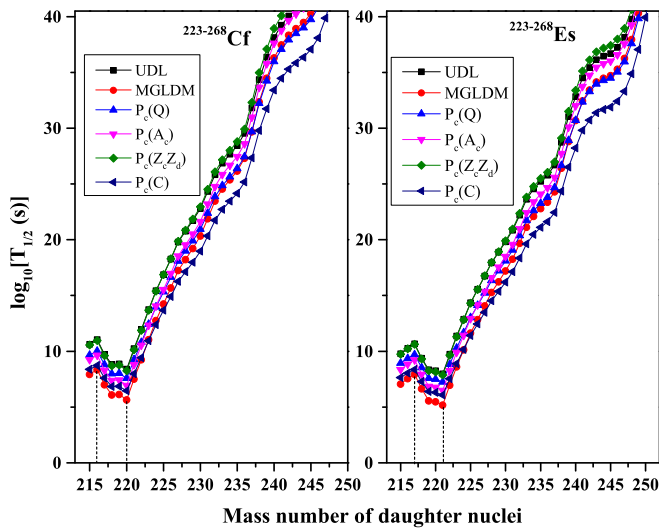
Given the validity of our results from $\alpha$ decay, we attempted to expand our investigation to double alpha decay as well. The double $\alpha$ decay of the isotopes of Pu, Am, Cm, Bk, Cf, Es, Fm, and Md in the mass region $A = 218$ to $273$ is also studied using MGLDM with the aid of different preformation factors.

Table II shows the comparison of half-lives of $2\alpha$ and $^8$Be emissions from $^{229}$Pu, $^{230}$Am, $^{232}$Cm, $^{234}$Bk, $^{236}$Cf, $^{239}$Es, $^{241}$Fm, and $^{245}$Md. $T_{1/2}^{\text{MGLDM}}$ in column 5 in Table II represents the logarithm of decay half-life in seconds estimated using MGLDM. $T_{1/2}^{(Q)}$, $T_{1/2}^{(A_c)}$, $T_{1/2}^{(Z_c Z_d)}$, and $T_{1/2}^{(C)}$ in columns 6–9 in Table II give the half-life determined using MGLDM with various preformation factors mentioned in Eqs. (11)–(14) given



FIG. 11. The variation of logarithm of half-life with the mass number of daughter nucleus for $2\alpha$ decay from $^{223-268}$Cf and $^{223-268}$Es.
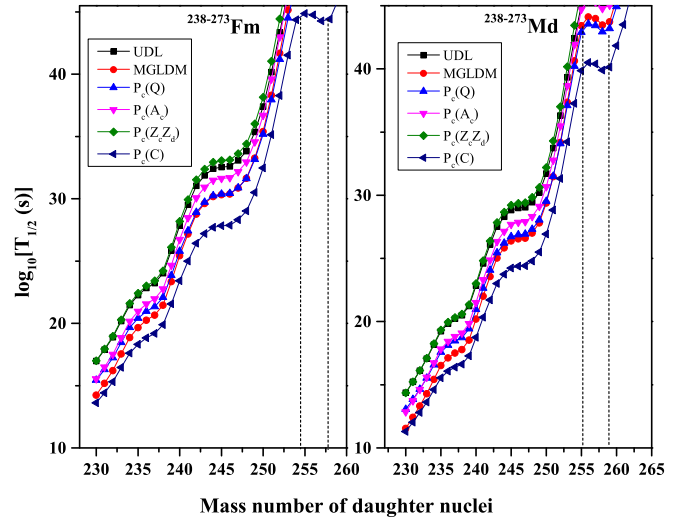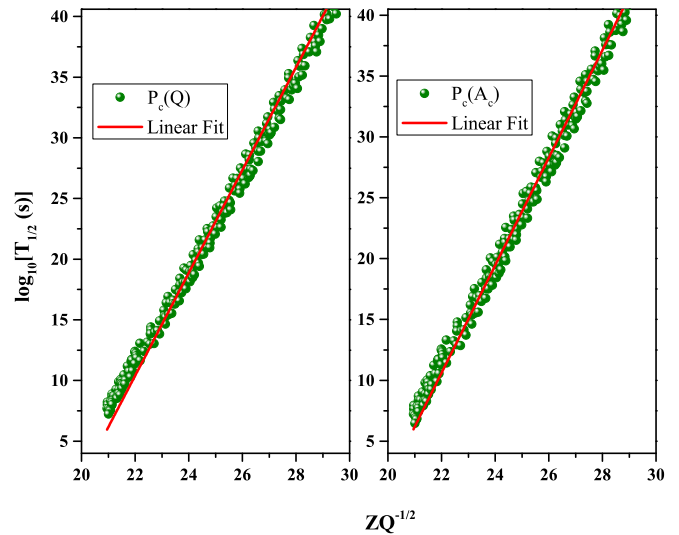


FIG. 13. The logarithm of $2\alpha$ half-life of all the isotopes calculated using $Q$ dependent preformation factor $P_c(Q)$ and cluster size dependent preformation factor $P_c(A_c)$ plotted against $ZQ^{-1/2}$.

TABLE III. The isotopes of Pu, Am, Cm, Bk, Cf, Es, Fm, and Md with the smallest double alpha decay half-lives.

| Parent nuclei | Daughter nuclei | Q Value (MeV) | $\log_{10}[T_{1/2} \text{ (s)}]$ | | | | | |
|---|---|---|---|---|---|---|---|---|
| | | | $T_{1/2}^{\text{MGLDM}}$ | $T_{1/2}^{(Q)}$ | $T_{1/2}^{(A_c)}$ | $T_{1/2}^{(Z_c Z_d)}$ | $T_{1/2}^{(C)}$ | $T_{1/2}^{\text{(UDL)}}$ |
| $^{218}\text{Pu}_{94}$ | $^{210}\text{Th}_{90}$ | 18.26777 | 11.260 | 12.398 | 12.558 | 13.629 | 11.231 | 13.751 |
| $^{219}\text{Pu}_{94}$ | $^{211}\text{Th}_{90}$ | 18.27667 | 11.199 | 12.339 | 12.498 | 13.568 | 11.174 | 13.699 |
| $^{220}\text{Pu}_{94}$ | $^{212}\text{Th}_{90}$ | 17.95257 | 12.013 | 13.077 | 13.312 | 14.382 | 11.864 | 14.499 |
| $^{221}\text{Pu}_{94}$ | $^{213}\text{Th}_{90}$ | 18.74137 | 9.947 | 11.195 | 11.245 | 12.316 | 10.098 | 12.489 |
| $^{222}\text{Pu}_{94}$ | $^{214}\text{Th}_{90}$ | 19.31437 | 8.520 | 9.902 | 9.818 | 10.889 | 8.889 | 11.097 |
| $^{223}\text{Pu}_{94}$ | $^{215}\text{Th}_{90}$ | 19.77767 | 7.407 | 8.897 | 8.705 | 9.776 | 7.952 | 10.009 |
| $^{224}\text{Pu}_{94}$ | $^{216}\text{Th}_{90}$ | 20.09387 | 6.659 | 8.223 | 7.958 | 9.028 | 7.324 | 9.279 |
| $^{225}\text{Pu}_{94}$ | $^{217}\text{Th}_{90}$ | 19.17847 | 8.735 | 10.086 | 10.034 | 11.104 | 9.053 | 11.327 |
| $^{226}\text{Pu}_{94}$ | $^{218}\text{Th}_{90}$ | 18.20107 | 11.140 | 12.262 | 12.438 | 13.509 | 11.085 | 13.688 |
| $^{227}\text{Pu}_{94}$ | $^{219}\text{Th}_{90}$ | 17.31877 | 13.495 | 14.409 | 14.793 | 15.863 | 13.102 | 15.988 |
| $^{228}\text{Pu}_{94}$ | $^{220}\text{Th}_{90}$ | 16.37477 | 16.241 | 16.933 | 17.539 | 18.609 | 15.485 | 18.658 |
| $^{218}\text{Am}_{95}$ | $^{210}\text{Pa}_{91}$ | 18.86467 | 10.449 | 11.726 | 11.747 | 12.88 | 10.532 | 12.984 |
| $^{219}\text{Am}_{95}$ | $^{211}\text{Pa}_{91}$ | 18.89637 | 10.333 | 11.617 | 11.631 | 12.763 | 10.428 | 12.877 |
| $^{220}\text{Am}_{95}$ | $^{212}\text{Pa}_{91}$ | 18.85077 | 10.408 | 11.682 | 11.707 | 12.839 | 10.486 | 12.959 |
| $^{221}\text{Am}_{95}$ | $^{213}\text{Pa}_{91}$ | 18.58917 | 11.031 | 12.243 | 12.329 | 13.461 | 11.009 | 13.574 |
| $^{222}\text{Am}_{95}$ | $^{214}\text{Pa}_{91}$ | 19.37057 | 9.066 | 10.461 | 10.365 | 11.497 | 9.342 | 11.658 |
| $^{223}\text{Am}_{95}$ | $^{215}\text{Pa}_{91}$ | 19.91267 | 7.765 | 9.286 | 9.063 | 10.196 | 8.245 | 10.386 |
| $^{224}\text{Am}_{95}$ | $^{216}\text{Pa}_{91}$ | 20.19717 | 7.087 | 8.674 | 8.385 | 9.517 | 7.674 | 9.724 |
| $^{225}\text{Am}_{95}$ | $^{217}\text{Pa}_{91}$ | 20.51677 | 6.347 | 8.008 | 7.645 | 8.778 | 7.055 | 9.001 |
| $^{226}\text{Am}_{95}$ | $^{218}\text{Pa}_{91}$ | 19.53027 | 8.542 | 9.974 | 9.841 | 10.973 | 8.878 | 11.170 |
| $^{227}\text{Am}_{95}$ | $^{219}\text{Pa}_{91}$ | 18.57837 | 10.838 | 12.049 | 12.136 | 13.269 | 10.813 | 13.427 |
| $^{228}\text{Am}_{95}$ | $^{220}\text{Pa}_{91}$ | 17.68157 | 13.181 | 14.181 | 14.479 | 15.612 | 12.813 | 15.719 |
| $^{229}\text{Am}_{95}$ | $^{221}\text{Pa}_{91}$ | 16.82317 | 15.609 | 16.408 | 16.908 | 18.040 | 14.912 | 18.084 |
| $^{223}\text{Cm}_{96}$ | $^{215}\text{U}_{92}$ | 20.00377 | 8.222 | 9.764 | 9.519 | 10.715 | 8.621 | 10.859 |
| $^{224}\text{Cm}_{96}$ | $^{216}\text{U}_{92}$ | 20.49267 | 7.086 | 8.741 | 8.384 | 9.579 | 7.669 | 9.747 |
| $^{225}\text{Cm}_{96}$ | $^{217}\text{U}_{92}$ | 20.71107 | 6.572 | 8.278 | 7.869 | 9.065 | 7.238 | 9.247 |
| $^{226}\text{Cm}_{96}$ | $^{218}\text{U}_{92}$ | 20.99897 | 5.919 | 7.691 | 7.217 | 8.412 | 6.693 | 8.607 |
| $^{227}\text{Cm}_{96}$ | $^{219}\text{U}_{92}$ | 19.95267 | 8.193 | 9.723 | 9.491 | 10.686 | 8.573 | 10.858 |
| $^{228}\text{Cm}_{96}$ | $^{220}\text{U}_{92}$ | 18.94957 | 10.562 | 11.859 | 11.860 | 13.055 | 10.563 | 13.191 |
| $^{229}\text{Cm}_{96}$ | $^{221}\text{U}_{92}$ | 18.08847 | 12.759 | 13.855 | 14.058 | 15.253 | 12.432 | 15.344 |
| $^{230}\text{Cm}_{96}$ | $^{222}\text{U}_{92}$ | 17.30767 | 14.901 | 15.813 | 16.199 | 17.394 | 14.275 | 17.434 |
| $^{231}\text{Cm}_{96}$ | $^{223}\text{U}_{92}$ | 16.67737 | 16.740 | 17.504 | 18.038 | 19.233 | 15.871 | 19.223 |
| $^{223}\text{Bk}_{97}$ | $^{215}\text{Np}_{93}$ | 19.85407 | 9.237 | 10.745 | 10.536 | 11.793 | 9.466 | 11.882 |
| $^{224}\text{Bk}_{97}$ | $^{216}\text{Np}_{93}$ | 20.56017 | 7.588 | 9.259 | 8.887 | 10.144 | 8.083 | 10.267 |
| $^{225}\text{Bk}_{97}$ | $^{217}\text{Np}_{93}$ | 20.99137 | 6.611 | 8.381 | 7.909 | 9.166 | 7.267 | 9.308 |
| $^{226}\text{Bk}_{97}$ | $^{218}\text{Np}_{93}$ | 21.06277 | 6.421 | 8.208 | 7.719 | 8.976 | 7.105 | 9.128 |
| $^{227}\text{Bk}_{97}$ | $^{219}\text{Np}_{93}$ | 21.32187 | 5.837 | 7.684 | 7.136 | 8.393 | 6.618 | 8.556 |
| $^{228}\text{Bk}_{97}$ | $^{220}\text{Np}_{93}$ | 20.32177 | 7.976 | 9.591 | 9.274 | 10.531 | 8.381 | 10.676 |
| $^{229}\text{Bk}_{97}$ | $^{221}\text{Np}_{93}$ | 19.45247 | 9.974 | 11.388 | 11.272 | 12.529 | 10.051 | 12.648 |
| $^{230}\text{Bk}_{97}$ | $^{222}\text{Np}_{93}$ | 18.64747 | 11.957 | 13.184 | 13.255 | 14.512 | 11.728 | 14.595 |
| $^{231}\text{Bk}_{97}$ | $^{223}\text{Np}_{93}$ | 17.91877 | 13.873 | 14.928 | 15.171 | 16.428 | 13.365 | 16.469 |
| $^{232}\text{Bk}_{97}$ | $^{224}\text{Np}_{93}$ | 17.32687 | 15.517 | 16.434 | 16.816 | 18.073 | 14.783 | 18.075 |
| $^{233}\text{Bk}_{97}$ | $^{225}\text{Np}_{93}$ | 16.78797 | 17.093 | 17.883 | 18.391 | 19.648 | 16.152 | 19.609 |
| $^{223}\text{Cf}_{98}$ | $^{215}\text{Pu}_{94}$ | 20.70907 | 7.948 | 9.653 | 9.246 | 10.565 | 8.384 | 10.636 |
| $^{224}\text{Cf}_{98}$ | $^{216}\text{Pu}_{94}$ | 20.50837 | 8.359 | 10.018 | 9.657 | 10.976 | 8.719 | 11.049 |
| $^{225}\text{Cf}_{98}$ | $^{217}\text{Pu}_{94}$ | 21.10617 | 7.005 | 8.802 | 8.303 | 9.622 | 7.589 | 9.720 |
| $^{226}\text{Cf}_{98}$ | $^{218}\text{Pu}_{94}$ | 21.52117 | 6.089 | 7.981 | 7.387 | 8.706 | 6.829 | 8.821 |
| $^{227}\text{Cf}_{98}$ | $^{219}\text{Pu}_{94}$ | 21.47817 | 6.142 | 8.024 | 7.439 | 8.759 | 6.867 | 8.880 |
| $^{228}\text{Cf}_{98}$ | $^{220}\text{Pu}_{94}$ | 21.69877 | 5.648 | 7.581 | 6.946 | 8.265 | 6.455 | 8.397 |
| $^{229}\text{Cf}_{98}$ | $^{221}\text{Pu}_{94}$ | 20.80257 | 7.518 | 9.245 | 8.817 | 10.136 | 7.989 | 10.255 |
| $^{230}\text{Cf}_{98}$ | $^{222}\text{Pu}_{94}$ | 20.02377 | 9.250 | 10.797 | 10548 | 11.868 | 9.428 | 11.968 |
| $^{231}\text{Cf}_{98}$ | $^{223}\text{Pu}_{94}$ | 19.26187 | 11.054 | 12.424 | 12.352 | 13.672 | 10.944 | 13.746 |
| $^{232}\text{Cf}_{98}$ | $^{224}\text{Pu}_{94}$ | 18.58107 | 12.764 | 13.975 | 14.062 | 15.381 | 12.394 | 15.424 |
| $^{233}\text{Cf}_{98}$ | $^{225}\text{Pu}_{94}$ | 18.01767 | 14.252 | 15.331 | 15.549 | 16.869 | 13.667 | 16.880 |
| $^{234}\text{Cf}_{98}$ | $^{226}\text{Pu}_{94}$ | 17.50237 | 15.677 | 16.635 | 16.975 | 18.295 | 14.896 | 18.273 |

TABLE III. *(Continued.)*

| Parent nuclei | Daughter nuclei | $Q$ Value (MeV) | $\log_{10}[T_{1/2} \text{ (s)}]$ | | | | | |
|---|---|---|---|---|---|---|---|---|
| | | | $T_{1/2}^{\text{MGLDM}}$ | $T_{1/2}^{(Q)}$ | $T_{1/2}^{(A_c)}$ | $T_{1/2}^{(Z_c Z_d)}$ | $T_{1/2}^{(C)}$ | $T_{1/2}^{(\text{UDL})}$ |
| $^{235}\text{Cf}_{98}$ | $^{227}\text{Pu}_{94}$ | 16.96297 | 17.247 | 18.078 | 18.545 | 19.864 | 16.258 | 19.801 |
| $^{223}\text{Es}_{99}$ | $^{215}\text{Am}_{95}$ | 21.40977 | 7.069 | 8.936 | 8.367 | 9.749 | 7.653 | 9.791 |
| $^{224}\text{Es}_{99}$ | $^{216}\text{Am}_{95}$ | 21.16787 | 7.551 | 9.362 | 8.849 | 10230 | 8.044 | 10.274 |
| $^{225}\text{Es}_{99}$ | $^{217}\text{Am}_{95}$ | 20.97227 | 7.939 | 9.706 | 9.238 | 10.619 | 8.359 | 10.666 |
| $^{226}\text{Es}_{99}$ | $^{218}\text{Am}_{95}$ | 21.55937 | 6.639 | 8.541 | 7.938 | 9.319 | 7.279 | 9.388 |
| $^{227}\text{Es}_{99}$ | $^{219}\text{Am}_{95}$ | 22.05897 | 5.571 | 7.587 | 6.869 | 8.250 | 6.397 | 8.336 |
| $^{228}\text{Es}_{99}$ | $^{220}\text{Am}_{95}$ | 22.08627 | 5.479 | 7.501 | 6.777 | 8.158 | 6.315 | 8.251 |
| $^{229}\text{Es}_{99}$ | $^{221}\text{Am}_{95}$ | 22.21107 | 5.191 | 7.242 | 6.489 | 7.871 | 6.074 | 7.972 |
| $^{230}\text{Es}_{99}$ | $^{222}\text{Am}_{95}$ | 21.33157 | 6.975 | 8.824 | 8.273 | 9.654 | 7.529 | 9.748 |
| $^{231}\text{Es}_{99}$ | $^{223}\text{Am}_{95}$ | 20.56967 | 8.616 | 10.289 | 9.914 | 11.296 | 8.885 | 11.376 |
| $^{232}\text{Es}_{99}$ | $^{224}\text{Am}_{95}$ | 19.89977 | 10.140 | 11.658 | 11.438 | 12.819 | 10.156 | 12.882 |
| $^{233}\text{Es}_{99}$ | $^{225}\text{Am}_{95}$ | 19.27407 | 11.639 | 13.012 | 12.937 | 14.319 | 11.418 | 14.358 |
| $^{234}\text{Es}_{99}$ | $^{226}\text{Am}_{95}$ | 18.78657 | 12.856 | 14.114 | 14.154 | 15.535 | 12.449 | 15.554 |
| $^{235}\text{Es}_{99}$ | $^{227}\text{Am}_{95}$ | 18.31647 | 14.077 | 15.226 | 15.376 | 16.757 | 13.492 | 16.753 |
| $^{236}\text{Es}_{99}$ | $^{228}\text{Am}_{95}$ | 17.86817 | 15.290 | 16.334 | 16.588 | 17.969 | 14.534 | 17.939 |
| $^{237}\text{Es}_{99}$ | $^{229}\text{Am}_{95}$ | 17.52347 | 16.249 | 17.212 | 17.547 | 18.928 | 15.360 | 18.877 |
| $^{238}\text{Es}_{99}$ | $^{230}\text{Am}_{95}$ | 17.18767 | 17.212 | 18.096 | 18.510 | 19.892 | 16.195 | 19.818 |
| $^{238}\text{Fm}_{100}$ | $^{230}\text{Cm}_{96}$ | 18.47577 | 14.249 | 15.436 | 15.548 | 16.991 | 13.610 | 16.6969 |
| $^{239}\text{Fm}_{100}$ | $^{231}\text{Cm}_{96}$ | 18.12117 | 15.195 | 16.298 | 16.493 | 17.936 | 14.420 | 17.896 |
| $^{240}\text{Fm}_{100}$ | $^{232}\text{Cm}_{96}$ | 17.75017 | 16.218 | 17.234 | 17.516 | 18.959 | 15.302 | 18.897 |
| $^{238}\text{Md}_{101}$ | $^{230}\text{Bk}_{97}$ | 19.78187 | 11.558 | 13.049 | 12.856 | 14.362 | 11.299 | 14.365 |
| $^{239}\text{Md}_{101}$ | $^{231}\text{Bk}_{97}$ | 19.41837 | 12.433 | 13.839 | 13.731 | 15.237 | 12.037 | 15.229 |
| $^{240}\text{Md}_{101}$ | $^{232}\text{Bk}_{97}$ | 19.05677 | 13.331 | 14.653 | 14.629 | 16.135 | 12.798 | 16.113 |
| $^{241}\text{Md}_{101}$ | $^{233}\text{Bk}_{97}$ | 18.68017 | 14.298 | 15.532 | 15.596 | 17.102 | 13.621 | 17.064 |
| $^{242}\text{Md}_{101}$ | $^{234}\text{Bk}_{97}$ | 18.25197 | 15.442 | 16.576 | 16.740 | 18.246 | 14.603 | 18.185 |
| $^{243}\text{Md}_{101}$ | $^{235}\text{Bk}_{97}$ | 17.86027 | 16.525 | 17.568 | 17.824 | 19.329 | 15.536 | 19.245 |
| $^{244}\text{Md}_{101}$ | $^{236}\text{Bk}_{97}$ | 17.63867 | 17.140 | 18.130 | 18.438 | 19.944 | 16.066 | 19.849 |

in Sec. II. $T_{1/2}^{(\text{UDL})}$ given in column 10 represents the UDL half-life predictions. Since the mass defect $^8\text{Be}$ is slightly greater than that of $2\alpha$, a larger $Q$ value and shorter half-life can be anticipated for $2\alpha$ decay than $^8\text{Be}$ emission. We can observe this by analyzing Table II. The half-lives for $2\alpha$ decay are less than that of $^8\text{Be}$ emission and as a result $2\alpha$ decay is more probable than $^8\text{Be}$ emission. Moreover, the possibility of $^8\text{Be}$ emission is less since it is a weakly bound nucleus.

In Fig. 9, the logarithms of decay half-lives computed using the MGLDM with different preformation factors and UDL for the $2\alpha$ decay of $^{218-258}\text{Pu}$ and $^{218-258}\text{Am}$ are plotted along the $y$ axis and the mass numbers of daughter nuclei are plotted along the $x$ axis. As depicted in Figs. 10–12, similar graphs are drawn for the $2\alpha$ decay of $^{223-268}\text{Cm}$, $^{223-268}\text{Bk}$, $^{223-268}\text{Cf}$, $^{223-268}\text{Es}$, $^{238-273}\text{Fm}$, and $^{238-273}\text{Md}$.

A peak and dip in half-life are observed at mass numbers 212 and 216, respectively, for the $2\alpha$ decay of $^{218-258}\text{Pu}$. The daughter nuclei contain 126 neutrons when the mass number of the daughter is 216 whereas the parent nuclei's neutron number is 126 when the daughter's mass number is 212. The same is true for the decay of $^{218-258}\text{Am}$, where maximum and minimum $T_{1/2}$ are found at mass numbers 213 and 217, respectively, as demonstrated in Fig. 9. In the case of $^{223-268}\text{Cm}$, half-life shows a minimum value at mass number 218 corresponding to magic neutron number 126. Figure 10 shows that for the double alpha decay of $^{223-268}\text{Bk}$, minimum $T_{1/2}$ is observed at mass number 219 when the daughter nuclei possess magic neutron number 126.

For mass number 220, representing neutron number 126, the least half-life is shown for $2\alpha$ decay from $^{223-268}\text{Cf}$. At mass number 216, when the parent nucleus contains 126 neutrons, the $2\alpha$ decay of Cf attains a maximum value for half-life. From Fig. 11, the least half-life for the decay of $^{223-268}\text{Es}$ is noted at mass number 221, which indicates neutron magic number 126. The decay half-life achieves maximum value at mass number 217 for $^{223-268}\text{Es}$, when the parent nuclei's neutron number is 126 whereas for $^{238-273}\text{Fm}$, maximum $T_{1/2}$ is observed at 254, when the parent nuclei's neutron number is 162. The analysis of Fig. 12 shows that the half-lives approach their minimum values at mass number 258 for the $2\alpha$ decay of $^{238-273}\text{Fm}$ and at mass number 259 for the $2\alpha$ decay of $^{238-273}\text{Md}$ corresponding to neutron number 162. Double alpha decay from $^{238-273}\text{Md}$ shows maximum $T_{1/2}$ at mass number 255, when the parent isotope has 162 neutrons. The observations from the double alpha decay of these isotopes are similar to those from alpha decay. The decay half-lives approach their maximum and minimum values when the parent nuclei and daughter nuclei, respectively, possess a magic number of neutrons.

Table III lists the isotopes having the shortest half-lives for double alpha decay. $T_{1/2}^{\mathrm{MGLDM}}$ in column 4 in Table II represents the logarithm of the decay half-life in seconds estimated using MGLDM. $T_{1/2}^{(Q)}$, $T_{1/2}^{(A_c)}$, $T_{1/2}^{(Z_c Z_d)}$, and $T_{1/2}^{(C)}$ in columns 5–8 in Table II give the half-life determined using MGLDM with various preformation factors mentioned in Eqs. (11)–(14) given in Sec. II. $T_{1/2}^{(\mathrm{UDL})}$ given in column 9 represents the UDL half-life predictions.

Due to their great probability of undergoing decay and likelihood of being observed experimentally, the isotopes with the shortest half-lives ($<10^{20}$ s) for double alpha decay are only highlighted in Table II. A proposal [14] has been submitted at the ISOLDE facility in CERN for probing the double alpha radioactivity of $^{224}$Ra. Hence there is a growing interest in investigating $2\alpha$ decay experimentally and we anticipate that our findings regarding the double alpha decay of these isotopes will be helpful while planning future double alpha decay experiments.

Additionally, we plotted the logarithms of $2\alpha$ decay half-lives of all the isotopes predicted by MGLDM with different preformation factors against $ZQ^{-1/2}$ and found them to be linear. The plots created using the $Q$ dependent preformation factor and the cluster size ($A_c$) dependent preformation factor are displayed in Fig. 13. All the plots are fitted into a straight line and the slope and intercept are obtained for each plot. The slopes obtained by using $P_c$ ($Q$), $P_c$ ($A_c$), $P_c$ ($Z_c Z_d$), and $P_c$ ($C$) are 4.2349, 4.4208, 4.4170, and 4.1240, respectively, whereas the corresponding intercepts are $-82.7736$, $-86.6510$, $-85.2593$, and $-81.9688$. The linear nature of the plots connecting $\log_{10} T_{1/2}$ versus $ZQ^{-1/2}$ stresses the reliability of our predictions using MGLDM with different preformation factors.

## IV. CONCLUSIONS

In our present paper we have studied the $\alpha$ decay and $2\alpha$ decay of different isotopes of Pu, Am, Cm, Bk, Cf, Es, Fm, and Md in the mass region $A = 218$ to 273 using MGLDM and UDL. We compared the $\alpha$ decay half-lives of these isotopes predicted using MGLDM and UDL with corresponding experimental data. With standard deviations of 1.18 and 1.20, respectively, the half-lives predicted using MGLDM and UDL are in good agreement with the experimental results, demonstrating the validity of our method. Consequently, we expanded our research to also examine the double alpha decay of these isotopes using MGLDM by utilizing different preformation factors. From our analysis, we concluded that minimum and maximum half-lives indicate the stability of daughter nuclei and parent nuclei, respectively. At neutron numbers 126 and 162 of the parent or daughter nuclei a peak or dip in half-lives is observed. The nuclei possess an extra stability at magic numbers 126 and 162. Hence the parent nuclei with magic neutron number will be stable against decay whereas the magic daughter nuclei will be formed with ease after undergoing decay, resulting in maximum and minimum $T_{1/2}$, respectively. Thus the magicity of the nucleus plays a significant role in the half-life of the nucleus. We have also obtained linear plots when $\log_{10} T_{1/2}$ of all the isotopes are plotted against $ZQ^{-1/2}$ which further proves the reliability of our calculations.

[1] P. R. Chowdhury, C. Samanta, and D. N. Basu, Phys. Rev. C **73**, 014612 (2006).

[2] V. Yu. Denisov and A. A. Khudenko, Phys. Rev. C **81**, 034613 (2010).

[3] B. Buck, A. C. Merchant, and S. M. Perez, Phys. Rev. C **45**, 2247 (1992).

[4] M. Goeppert-Mayer, Phys. Rev. **48**, 512 (1935).

[5] E. Beardsworth, R. Hensler, J. W. Tape, N. Benczer-Koller, W. Darcey, and J. R. MacDonald, Phys. Rev. C **8**, 216 (1973).

[6] K. P. Santhosh, Phys. Rev. C **104**, 064613 (2021).

[7] Z. Kohley, T. Baumann, D. Bazin, G. Christian, P. A. DeYoung, J. E. Finck, N. Frank, M. Jones, E. Lunderberg, B. Luther, S. Mosby, T. Nagi, J. K. Smith, J. Snyder, A. Spyrou, and M. Thoennessen, Phys. Rev. Lett. **110**, 152501 (2013).

[8] D. N. Poenaru and M. Ivascu, J. Physique Lett. **46**, 591 (1985).

[9] V. I. Tretyak, Nucl. Phys. At. Energy **22**, 121 (2021).

[10] P. de Marcillac, N. Coron, G. Dambier, J. Leblance, and J. P. Moalic, Nature (London) **422**, 876 (2003).

[11] F. Mercier, J. Zhao, J.-P. Ebran, E. Khan, T. Nikšić, and D. Vretenar, Phys. Rev. Lett. **127**, 012501 (2021).

[12] K. P. Santhosh and Tinu Ann Jose, Phys. Rev. C **104**, 064604(2021).

[13] V. Yu. Denisov, Phys. Lett. B **835**, 137569 (2022).

[14] Ch. Theisen and E. Khan, CERN-INTC Proposal No. 2022-016 /INTC-CLL-049, 2022 (unpublished).

[15] G. Royer and B. Remaud, J. Phys. G: Nucl. Part. Phys. **10**, 1057 (1984).

[16] G. Royer and B. Remaud, Nucl. Phys. A. **444**, 477 (1985).

[17] J. Blocki, J. Randrup, W. J. Swiatecki, and C. F. Tsang, Ann. Phys. (NY) **105**, 427 (1977).

[18] K. P. Santhosh, C. Nithya, H. Hassanabadi, and D. T. Akrawy, Phys. Rev. C **98**, 024625 (2018).

[19] K. P. Santhosh, C. Nithya, and Tinu Ann Jose, Phys. Rev. C **104**, 024617 (2021).

[20] K. P. Santhosh and Tinu Ann Jose, Phys. Rev. C **99**, 064604 (2019).

[21] K. P. Santhosh and Tinu Ann Jose, Nucl. Phys. A. **992**, 121626 (2019).

[22] K. P. Santhosh and Tinu Ann Jose, Indian J. Phys. **95**, 121 (2021).

[23] K. P. Santhosh and Tinu Ann Jose, Pramana **95**, 162 (2021).

[24] J. Blocki and W. J. Swiatecki, Ann. Phys. (NY) **132**, 53 (1981).

[25] C. Qi, F. R. Xu, R. J. Liotta, and R. Wyss, Phys. Rev. Lett. **103**, 072501 (2009).

[26] N. Wang, M. Liu, X. Wu, and J. Meng, Phys. Lett. B **734**, 215 (2014).

[27] M. Wang, W. J. Huang, F. G. Kondev, G. Audi, and S. Naimi, Chinese Phys. C **45**, 030003 (2021).

[28] F. G. Kondev, M. Wang, W. J. Huang, S. Naimi, and G. Audi, Chin. Phys. C **45**, 030001 (2021).